

# LIFE IN THE BUBBLE: HOW A NEARBY SUPERNOVA LEFT EPHEMERAL FOOTPRINTS ON THE COSMIC-RAY SPECTRUM AND INDELIBLE IMPRINTS ON LIFE

CAITLYN NOJIRI<sup>1</sup>, NOÉMIE GLOBUS<sup>1,2,3</sup>, AND ENRICO RAMIREZ-RUIZ<sup>1</sup>

<sup>1</sup>Department of Astronomy and Astrophysics, University of California, Santa Cruz, CA 95064, USA

<sup>2</sup>Kavli Institute for Particle Astrophysics and Cosmology, Stanford University, Stanford, CA 94305, USA

<sup>3</sup>Astrophysical Big Bang Laboratory, RIKEN, Wako, Saitama, Japan

## ABSTRACT

The Earth sits inside a 300pc-wide void that was carved by a series of supernova explosions that went off tens of millions of years ago, pushing away interstellar gas and creating a bubble-like structure. The <sup>60</sup>Fe peak deposits found in the deep-sea crust have been interpreted by the imprints left by the ejecta of supernova explosions occurring about 2-3 and 5-6 Myr ago. It is likely that the <sup>60</sup>Fe peak at about 2-3 Myr originated from a supernova occurring in the Upper Centaurus Lupus association in Scorpius Centaurus ( $\approx 140$  pc) or the Tucana Horologium association ( $\approx 70$  pc). Whereas, the  $\approx 5$ -6 Myr peak is likely attributed to the solar system's entrance into the bubble. In this *Letter*, we show that the supernova source responsible for synthesizing the <sup>60</sup>Fe peak deposits  $\approx 2$ -3 Myr ago was also likely a Galactic PeVatron source. We demonstrate that this supernova can consistently explain the “knee” in the cosmic-ray spectrum and the large-scale anisotropy between 100 TeV and 100 PeV. Matching the intensity and shape of the cosmic-ray spectrum allows us to place stringent constraints on the cosmic-ray energy content from the supernova as well as on the cosmic-ray diffusion coefficient. Making use of such constraints we provide a robust estimate of the temporal variation of terrestrial ionizing cosmic radiation levels and discuss their implications in the development of early life on Earth by plausibly influencing the mutation rate and, as such, conceivably assisting in the evolution of complex organisms.

*Keywords:* High-energy cosmic radiation (731); Superbubbles (1656); Cosmic ray astronomy (324); Astrobiology (74), Supernovae (1668); Ejecta (453); Astronomical radiation sources (89)

## 1. INTRODUCTION

Life on Earth is constantly evolving under continuous exposure to ionizing radiation from both terrestrial and cosmic origin. While bedrock radioactivity slowly decreases on billion year timescales (Karam & Leslie 1999; Nimmo et al. 2020), the levels of cosmic radiation fluctuates as our solar system travels through the Milky Way. Nearby supernova (SN) activity has the potential to raise the radiation levels at the surface of the Earth by several orders of magnitude, which is expected to have a profound impact on the evolution of life (Ellis & Schramm 1995). In particular, enhanced radiation levels are expected when our solar system passes near OB associations. The winds associated with these massive stellar factories are expected to initially inflate superbubbles of hot plasma, which can be the birth places of a large fraction of the core collapse explosions taking place within the OB association (Lingenfelter 2018). The solar system entered such a superbubble, commonly referred to as the Local Bubble (LB), about 6 Myr ago, and currently resides near

its center (Zucker et al. 2022). The presence of freshly synthesized radioisotopes detected near the Earth's surface gives credence to the idea that our Solar System has infiltrated a highly active SN region within the the Milky Way (Benítez et al. 2002; Ertel et al. 2023). Most notably, the temporal variation in the concentration of <sup>60</sup>Fe in sediment and crust regions (Wallner et al. 2021) places stringent constraints on the positions and ages of the closest SN events (Fry et al. 2015; Hyde & Pecauc 2018; Zucker et al. 2022).

In this *Letter* we combine recent results on the properties of the LB and the detection of <sup>60</sup>Fe in deep-sea sediments to predict the cosmic-ray flux expected from a near-Earth core collapse SN event. We suggest that a single local PeVatron source, likely originating from the Scorpius Centaurus or the Tucana Horologium stellar associations, was responsible for the producing most of the freshly synthesized <sup>60</sup>Fe peak  $\approx 2.5$  Myr. We then proceed to calculate the associated cosmic-ray flux. This suggestion is given further credence by recent measurements of the cosmic-ray spectrum, composition, and

large-scale anisotropy. Motivated by the derived source constraints, our goal is to provide a robust estimate of the temporal variations of cosmic-ray radiation doses experienced by Earth’s inhabitants, using all available observational constraints. This *Letter* is organized as follows. In Section 2, we detail recent observational results that constrain the parameters of our cosmic-ray injection model, which is described in Section 3. Our results and their match to observational constraints are presented in Section 4. Our conclusions are submitted in Section 5.

## 2. OBSERVATIONAL CONSTRAINTS

In this section we present a summary of what we have learnt so far about the near-Earth massive stellar associations. We show that sufficient progress has been made in order to identify the necessary ingredients needed to estimate the history of cosmic-ray irradiation of our planet. The following questions were used to guide the assembly of these essential ingredients into a general model scheme.

### 2.1. *What nearby stellar associations are thought to dominate the ongoing SN activity?*

The nearest active star-forming region to the Sun is the  $\approx 15$ -Myr-old OB association Scorpius Centaurus (Sco-Cen). It is thought to be responsible for most of the massive stellar activity that conceived the LB (Frisch et al. 2011; Zucker et al. 2022). The associated SN activity in Sco-Cen is also credited with creating the Loop I superbubble which has been observed to interact and subsequently merge with the LB (Egger & Aschenbach 1995). Not to mention that our solar system is conjectured to be currently traversing an outflow originating from Sco-Cen (Piecka et al. 2024).

At present OB Sco-Cen association spans distances between 100 and 150 pc and includes several molecular clouds currently undergoing star formation (Ratzenböck et al. 2023). Sco-Cen is divided into three subgroups: the Lower Centaurus Crux (LCC), Upper Centaurus Lupus (UCL) and Upper Scorpius (US). Another highly viable candidate for hosting a near-Earth SN is the  $\approx 40$  Myr-old Tucana-Horologium (Tuc-Hor, Galli et al. 2023; Hyde & Pecaut 2018) association, one of the closest young stellar groups to the Solar System with an average distance of about 46 pc. A layout (*left* panel) and a sky map (*right* panel) of the LB and nearby stellar associations is shown in Figure 1. We foresee an anisotropy in the distribution of arrival directions of cosmic rays associated with a SN explosion residing in these nearby stellar associations.

### 2.2. *Which stellar association is most likely to be responsible the latest SN event?*

The LB is expected to have been inflated by a combination of stellar winds and SN explosions (e.g., Rosen et al. 2014). These SN blast waves can disperse freshly synthesised elements that can then be turbulently mixed (Gallegos-Garcia

et al. 2020; Kolborg et al. 2022, 2023) throughout the LB. This is expected to be the case for the freshly synthesised dust composed of proto-silicates, silicon dioxide and iron oxide, containing the radioactive isotope  $^{60}\text{Fe}$  that was captured by the Earth and incorporated into the geological record. Peak concentrations of  $^{60}\text{Fe}$  occurred about 2-3 Myr ago and 6-7 Myr ago (Wallner et al. 2021).

Constraints on the birth-site of the supernova progenitors responsible for these two main peaks can be placed from the initial mass function (IMF), the ages of nearby stellar groups and the metal dispersion time across the LB. The transport timescales expected if  $^{60}\text{Fe}$  was entrained in the supernova blast wave plasma are  $\lesssim 0.1$  Myr (Kolborg et al. 2022) and  $\lesssim 1$  Myr if  $^{60}\text{Fe}$  arrived in the form of supernova dust, whose dynamics differ from but are connected to the evolution of the blast wave material (Ertel et al. 2023). As such, it is believed that the radioactive age can be effectively used to constraint the time since explosion. Sco-Cen entered the LB  $\approx 10$  Myr ago (Fuchs et al. 2006; Maíz-Apellániz 2001; Ratzenböck et al. 2023) and since then, a handful of SN explosions have been predicted to occur in this association (Fuchs et al. 2006). According to Hyde & Pecaut, UCL and LCC remain plausible sites for hosting the event responsible for producing the  $^{60}\text{Fe}$  peak concentration 2-3 Myr ago. Both LCC and UCL contain prospective progenitors with initial mass estimates  $\gtrsim 20M_{\odot}$ .

Another hint for a progenitor site relates to the discovery of a new Galactic “bubble”, of radial extend 45 pc located at a distance of  $\approx 140$  pc in the UCL (Robitaille et al. 2018). This remnant is shown in Figure 1, and can be identified under the label “bubble”. The radial extension of the remnant is consistent with one SN going off inside the rarefied LB medium (Weaver et al. 1977). Not only that, the  $\approx 3$  Myr old runaway pulsar PSR J1932+1059 and the runaway O star  $\zeta$  Oph are both likely associated with a SN event in the UCL. Both stellar objects are estimated to have left the UCL subgroup about 3 Myr ago (Hoogerwerf et al. 2000). All these observations give credibility to the idea that SN activity in the UCL could have been responsible for producing the  $^{60}\text{Fe}$  peak 2-3 Myr ago.

The stellar cluster Tuc-Hor, on the other hand, is expected to have produced about a single SN since the Sun entered the LB about 6 Myr ago. A Salpeter IMF predicts  $\approx 1$  star with mass  $> 8 M_{\odot}$  which would have evolved into core collapse in the recent past (Mamajek 2016). Tuc-Hor association can not be ruled out as a candidate of the 2-3 Myr or the 6-7 Myr  $^{60}\text{Fe}$  peaks. However, since Tuc-Hor is the oldest, Hyde & Pecaut suggest the UCL association as the most likely site for the 2-3 Myr  $^{60}\text{Fe}$  peak. Another possible explanation for the 6-7 Myr  $^{60}\text{Fe}$  peak is attributed to the Solar System traversing the denser shell region of the LB (Fang et al. 2020). In absence of more stringent constraints, in what follows we consider both the Tuc-Hor cluster and the Sco-Cen’s UCL subgroup as likely candidates for the production of the 2-3 Myr  $^{60}\text{Fe}$

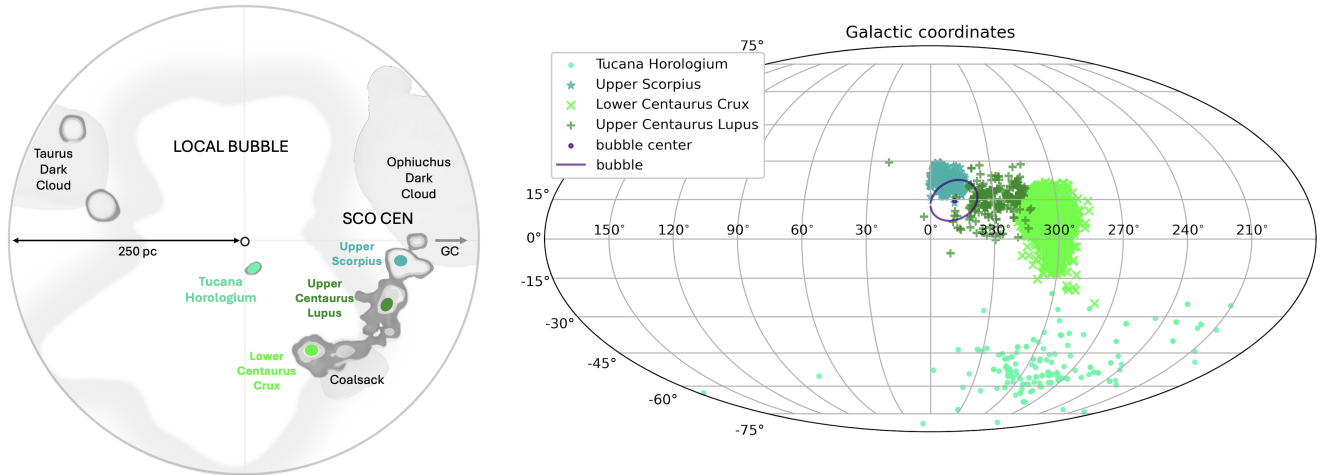


**Figure 1.** The configuration of stellar associations in and around the LB. *Left panel:* Shown is a map of today’s LB and the locations of the nearby stellar associations. The shape of the LB is taken from (Zucker et al. 2022). *Right panel:* Shown are the positions in Galactic coordinates of the nearby stellar associations Tuc-Hor and Sco-Cen’s subgroups: Lower Centaurus Crux (LCC), Upper Centaurus Lupus (UCL), and Upper Scorpius (US). Also shown (*bubble*) is the new Galactic bubble discovered by Robitaille et al. (2018), which is likely the remnant of a supernova that took place in UCL. We anticipate an anisotropy in the distribution of arrival directions of cosmic rays that results from SN explosions hosted by these nearby stellar associations.

deposits.

### 2.3. What can be learned from cosmic-ray data?

One of the key features in the cosmic-ray spectrum is the “knee” observed at around  $\approx 5$  PeV, where the power spectral index changes from 2.7 to 3.3. The presence of a clear succession of “heavy knees”<sup>1</sup> at high energies suggest that a source with a single maximal rigidity<sup>2</sup> (5-6 PV) is dominating the spectrum in this region, just before the transition to the extragalactic cosmic ray contribution taking place at around 100 PeV (Globus et al. 2015). This is supported by the phase-flip in the dipole anisotropy at around 100 TeV in the Galactic center direction (e.g., Fujii 2024). Motivated by this, we surmise that a lone PeVatron source should be able to explain the spectrum, composition, and anisotropy in the 100 TeV-100 PeV range, and conjecture that the same source was likely the same SN responsible for producing the 2-3 Myr  $^{60}\text{Fe}$  peak. In fact, PeV acceleration is alleged to be efficient during the early SN stages (e.g., Cristofari 2021) and SN remnants exploding in hot bubble environments have been proposed as viable candidate sources for energies above PeV (Vieu & Reville 2023).

Our LB is not unique. The interstellar medium in the Milky Way disk is filled with plenty of superbubbles, believed to be the remnants of past collective supernova activity. The studies of these superbubbles can help shed light on how our LB

<sup>1</sup> A proton knee observed at  $\approx 5$  PeV, followed by a Helium at 10 PeV (Alemanno et al. 2024), a Silicon-like peak at around 50 PeV, and an Iron at around 100 PeV (Apel et al. 2011; Kuznetsov et al. 2024). The latest knee at  $\approx 400$  PeV marks the end of the ultra-heavy cosmic-ray component (Hörandel 2003).

<sup>2</sup> Rigidity in good approximation for ultra-relativistic particles can be defined as  $R = \frac{E}{Z}$ , where  $E$  is the total energy and  $Z$  is the charge.

was carved. Recently, LHAASO discovered a giant  $\gamma$ -ray bubble structure in the Cygnus star-forming region with photon energies above 100 TeV, clearly indicative of acceleration of protons up to PeV energies in a region containing a massive stellar OB association (Lhaaso Collaboration 2024). The total energy cosmic-ray content in all the cosmic rays presently filling the Cygnus superbubble is constrained from Fermi observations to be  $1.3\text{-}6.5 \times 10^{49}$  erg (Ackermann et al. 2011). Individual SNRs are consistent with similar cosmic-ray energy content based on  $\gamma$ -ray observations (Allen 1999). On that account, in what follows, we consider a total cosmic-ray injection energy per SN  $\approx 10^{49}$  erg.

### 2.4. How far from Earth were the clusters progenitor candidates at the time of the SN explosion?

Over the past  $\approx 6$  Myr, the sun traveled through the LB and, as such, the distance of the embedded stellar clusters to Earth has evolved with time. In order to understand the evolution of the clusters in relationship to the Earth we use data from Benítez et al. (2002) and Schulreich et al. (2023). The distance of the centers of the stellar associations as a function of time are shown in Figure 2. The uncertainties in the distance range estimates for LCC, US, UCL, and Tuc-Hor were used to calculate the corresponding uncertainties assuming Gaussian distributions, with the shaded regions in Figure 2 corresponding to  $\pm 2\sigma$ . At 2.5 Myr, the core of Tuc-Hor was  $\approx 70$  pc away while the core of UCL was  $\approx 140$  pc. In what follows, these are the distance estimates we consider for the SN event that produced the early  $^{60}\text{Fe}$  deposits.

## 3. MODEL ASSUMPTIONS AND METHODS

### 3.1. Assumptions

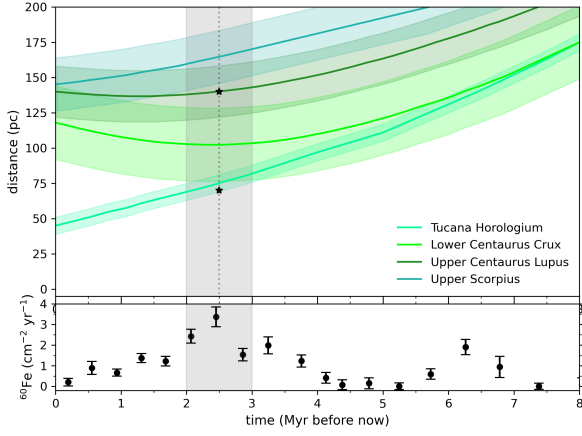


**Figure 2.** The distance from Earth to the clusters progenitor candidates. *Upper panel:* The evolution of our distance to the various stellar associations in time, which has been adapted from Benítez et al. (2002). The distance spread of the stellar associations is shown as shaded regions, which correspond to the associated  $2\sigma$  uncertainties in the distance estimate. The color code for the different associations is the same as in Figure 1. *Lower panel:* The collected data of  $^{60}\text{Fe}$ , which shows the two distinct peaks and has been adapted from Wallner et al. (2021). The shaded vertical grey region shows the most recent peak concentration at about 2-3 Myr. The width in peak times is thought to be produced by the transport timescales expected for  $^{60}\text{Fe}$  supernova dust (Ertel et al. 2023). The two black star symbols show the two SN progenitor candidates we consider in light of the observational constraints. These are located at a distance from Earth  $r_{\text{inj}} = 70$  pc at  $t_{\text{inj}} = 2.5$  Myr in Tucana Horologium, and  $r_{\text{inj}} = 140$  pc at  $t_{\text{inj}} = 2.5$  Myr in Upper Centaurus Lupus.

Motivated by the recent mapping of the star forming regions within the LB, we consider either Tuc-Hor or Sco-Cen’s UCL subgroup as likely hosts for the 2-3 Myr  $^{60}\text{Fe}$  SN event. We consider that this event acted as a PeVatron source, and is also responsible for the “knee” feature in the cosmic ray spectrum. We then make the natural assumption that all accelerated nuclei have the same spectrum in rigidity and simply determine the relative abundances from the observational data. The light (p+He) data is taken from DAMPE (Alemanno et al. 2024), EAS-TOP (Aglietta et al. 2004), ARGO-YBJ (Bartoli et al. 2015), and KASCADE (Antoni et al. 2005). The heavy (Si+Fe) data is taken from Kang et al. (2023). We use data from HAWC (Morales-Soto & Arteaga-Velázquez 2022), Tibet-III (Amenomori et al. 2008) and KASCADE-Grande (Kang et al. 2023) to constraint the all-particle spectrum. The source spectrum needs to be steep enough so that the contribution of the local PeVatron does not exceed  $\lesssim 10\%$  of the flux at 1 GeV (Moskalenko, private com.)

To model the cosmic-ray transport from the SN to Earth, we need to understand the properties of the magnetic field in the LB. Many attempts have been made to constrain the local diffusion coefficient from secondary cosmic ray data. Below 200 GV rigidity, the data can be well-accounted for

with a single power-law form of the diffusion coefficient:  $D(R) = D_0(R/10\text{GV})^\eta$ , where the parameter  $\eta$  governs the evolution with rigidity, which is related to the underlying assumption on the turbulence spectrum. This parameter has been recently constrained by the DAMPE Collaboration to be  $\approx 0.477$ , which is very close to the prediction of the Kraichnan theory of turbulence (Dampe Collaboration 2022). Herbst et al. (2012) estimated the diffusion coefficient in the outer heliosheath to be consistent with several  $10^{26}$  to  $10^{27}$   $\text{cm}^2 \text{s}^{-1}$  at 1 GV. Recent TeV observations made by HAWC has demonstrated that the diffusion coefficient in tens of parsecs around nearby pulsars is two order of magnitude lower when compared to the rest of the interstellar medium (Abeysekara et al. 2017). They find  $D(100 \text{ TeV}) = 4.5 \times 10^{27} \text{ cm}^2 \text{ s}^{-1}$ , implying  $\approx 10^{26} \text{ cm}^2 \text{ s}^{-1}$  at 10 GV for a Kraichnan spectrum.

Motivated by these findings, our model assumptions are listed below.

- We consider two progenitor candidates: a SN with explosion coordinates  $(t_{\text{inj}}, r_{\text{inj}}) = (2.5 \text{ Myr}, 70 \text{ pc})$  for Tuc-Hor, and a SN with explosion coordinates  $(2.5 \text{ Myr}, 140 \text{ pc})$  for UCL. We assume both inject  $\approx 10^{49}$  erg in cosmic rays (we will allow variations of a factor 3 around this value to fit the knee).
- We assume all nuclei have the same spectrum in rigidity  $dN/dR \propto R^{-\alpha}$  up to an exponential cutoff in  $\exp(-R/R_{\text{cut}})$  with  $R_{\text{cut}} \approx 5 \text{ PV}$  to fit the knee. From this, we directly determine the slope,  $\alpha$ , and the relative abundances of the different elements from the observational data.
- We assume a functional form for the diffusion coefficient  $D(R) = D_0 (R/10\text{GV})^\eta$ , with values of  $D_0$  between  $10^{26}$  and  $10^{27} \text{ cm}^2 \text{ s}^{-1}$  and  $\eta = 0.5$ .

In the sections that follow we describe in detail the components of the numerical model used to calculate the cosmic-ray transport from the source to the Earth and then the radiation doses experienced at various atmospheric depths. To do this, we first calculate the flux at the top of the atmosphere by solving the diffusion of the primary cosmic rays.

### 3.2. Cosmic-ray intensity at the top of the atmosphere

The cosmic ray intensity contribution is given by

$$J_p(E, r, t) = \frac{c}{4\pi} f, \quad (1)$$

where  $f(E, r, t)$  is the distribution function of protons at time  $t$  and radial distance  $r$  from the source, which, in turn, satisfies the radial-temporal-energy dependent diffusion equation

$$(\partial f / \partial t) = (D(E)/r^2)(\partial / \partial r)r^2(\partial f / \partial r) + (\partial / \partial E)(Pf) + Q, \quad (2)$$

where we use spherical coordinates, with  $r$  being the radial distance from a given accelerator,  $P$  representing the energy losses and  $Q$  the injection term for cosmic rays. We assume that the proton energy loss  $P$  is due to nuclear interactions. The nuclear loss rate is  $P_{\text{nuc}} = E/\tau_{pp}$ , with  $\tau_{pp} = (n_p c \kappa \sigma_{pp})^{-1}$  is the timescale for the corresponding nuclear loss,  $\kappa \approx 0.45$  is the inelasticity of the interaction and  $\sigma_{pp}$  is the inelastic cross section for  $pp$  interactions. Above  $E_{\text{lab}} = 3$  GeV,  $\sigma_{pp}$  can be written as  $\sigma_{pp}(E_{\text{lab}}) = 30.364 - 1.716 \log(E_{\text{lab}}) + 0.981 \log(E_{\text{lab}})^2$  mb, assuming EPOS-LHC for the hadronic interaction model.

A solution to the diffusion equation for an arbitrary energy loss term, a fixed diffusion coefficient, and an impulsive injection spectrum  $f_{\text{inj}}(E)$ , such that  $Q(E, r, t) = N_0 f_{\text{inj}}(E) \delta(r_{\text{inj}}) \delta(t_{\text{inj}})$ , can be found for the particular case in which  $D(E) \propto E^\eta$  and  $f_{\text{inj}} \propto E^{-\alpha}$ . Under such conditions, the solution to the diffusion equation (Aharonian & Atoyan 1996) can be written as

$$f(E, r, t) \approx \frac{N_0 E^{-\alpha}}{(\pi^{3/2} r_{\text{diff}}^3)} \exp\left[-(\alpha - 1)t/\tau_{pp} - (r/r_{\text{diff}})^2\right], \quad (3)$$

where

$$r_{\text{diff}} = 2 \sqrt{D(E)t \frac{\exp(t\eta/\tau_{pp}) - 1}{(t\eta/\tau_{pp})}} \quad (4)$$

denotes the radius of the sphere up to which the particles of energy  $E$  have time to diffuse after being injected. We use this solution to calculate the cosmic ray spectrum at the top of the atmosphere for our two progenitor candidates at various times following the SN explosion. We then use these spectra as an input to calculate the radiation doses experienced at different depths in the atmosphere and underground. We describe the dose calculation procedure in the following section.

### 3.3. Atmospheric and underground fluxes

Here we follow the same procedure as the one described in Globus et al. (2021). The differential particle fluxes  $\Phi(E, X)$ , where  $E$  is the kinetic energy and  $X(h) = \int_h^\infty d\ell \rho(\ell)$  is the slant depth in  $\text{g}/\text{cm}^2$ , are computed using the one-dimensional cascade equation solver MCEq<sup>3</sup> (Fedynitch et al. 2015) with a kinetic energy range down to 10 MeV. The numerical routines from Meighen-Berger & Li (2019) are used to calculate the electromagnetic cross sections. Ionization losses  $\langle dE/dX \rangle$  are based on tables from (Berger et al. 2017; Particle Data Group 2020) and are tracked for each charged particle.

The present flux of cosmic rays is considered to be isotropic and represented by the Global Spline Fit (GSF) (Dembinski et al. 2017), which is a modern parameterization of the cosmic ray flux between rigidity of a few GV and

the highest observed energies at Earth. The omission of the planetary magnetic field and solar modulation effects affecting the spectrum below a few GV/nucleon is not expected to qualitatively change our results.

The absorbed dose rate  $d$  in Gy/s is calculated from the differential fluxes  $\Phi$  with the default units  $(\text{GeV cm}^2 \text{s sr})^{-1}$  using

$$d(X) = 2\pi \sum_p \int_{\cos \theta_{\text{max}}}^1 d \cos \theta \int dE_p \Phi_p(E_p, X) \left\langle \frac{dE_p}{dX} \right\rangle (E_p),$$

where  $\theta_{\text{max}} = \max(\pi/2, \pi - \arcsin[r_\oplus/(r_\oplus + h)])$ . Here  $h$  is the altitude above ground and  $r_\oplus$  is the radius of the planet. The index  $p$  iterates over the various particle species, while the expression for  $\cos \theta_{\text{max}}$  takes into account that at higher altitudes, particle cascades can develop upwards relative to the horizon. The model of the Earth's atmosphere used here is the Standard Atmosphere (1976). The reader is refer to Globus et al. (2021) for further details.

## 4. RESULTS

In this section, we show the results obtained with the using the formalism described above and setting  $\alpha \approx 1.8$ ,  $E_{\text{cut}} = 6$  PeV,  $D(E) = D_0 E^{0.5}$  with  $10^{26.5} \leq D_0 \leq 10^{27} \text{ cm}^2 \text{ s}^{-1}$ . The total energy injected is assumed to vary from  $N_0 = 10^{49}$  erg to  $N_0 = 3 \times 10^{49}$  erg depending on the value selected for the diffusion coefficient. A composition of  $\approx 90\%$  light (H+He),  $\approx 10\%$  CNO,  $\lesssim 1\%$  Si+Fe, and  $\lesssim 0.5\%$  r-process elements, provide a good fit to the elemental contributions to the observed spectrum in the 100 TeV-100 PeV energy range.

Figures 3 and 4 present the cosmic-ray spectra (*upper panels*) and the corresponding radiation doses (*lower panels*) experienced at different altitudes/depths on Earth. These are shown as a function of time, starting from the moment of the SN explosion to present day. It can be seen that the light and heavy components of our model provide a reasonable description of the data in the 100 TeV-100 PeV energy range. At lower and higher energies, other sources, as expected, dominate the flux as suggested by the anisotropy data (Fujii 2024). We do not aim to account for the proton ‘‘10 TeV bump’’ which has been recently suggested to be a re-acceleration feature by local stellar winds (Malkov & Moskalenko 2022). As can be seen from Figures 3 and 4, our PeVatron starts to dominate the flux  $\gtrsim 100$  TeV and its contribution ends at the ankle. Values of  $\alpha$  around  $\approx 1.8$  allow the PeVatron component to become very low to negligible at 10 TeV.

The ‘‘light ankle’’ observed by KASCADE-Grande can be naturally understood as the emergence of a light extragalactic component, taking over at around 100 PeV (Globus et al. 2015). The *dotted purple* line is used to show the combined light PeVatron+extragalactic component, which nicely reproduces the light ankle around 100 PeV. The *dotted red* line show the fit to the heavy knee which constrain the Si+Fe contribution of our local PeVatron source to be  $\lesssim 1\%$ . In

<sup>3</sup> <https://github.com/afedynitch/MCEq> (Version 1.3)

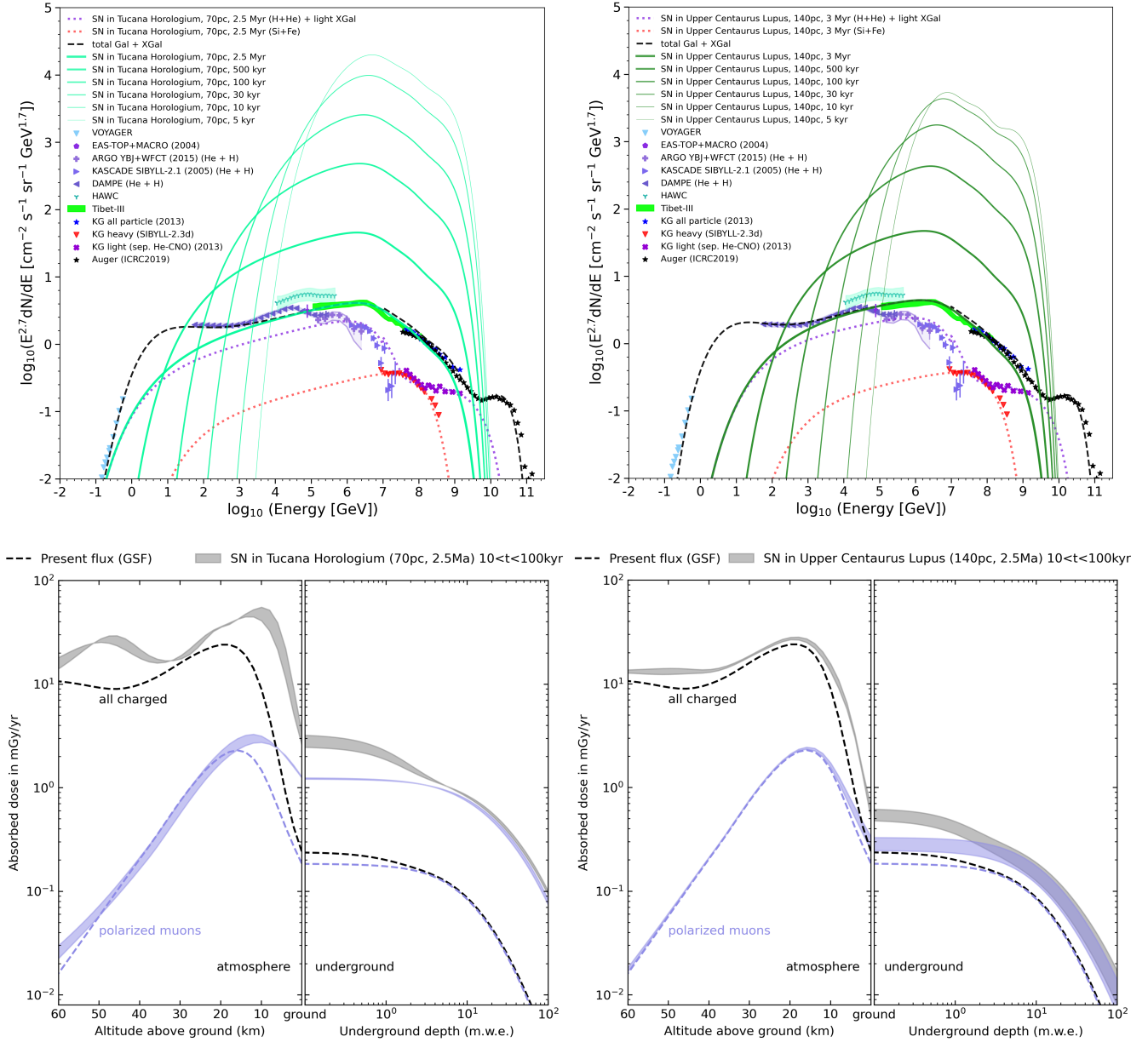


**Figure 3.** The cosmic-ray spectrum (*upper panels*) and the corresponding radiation dose experienced at different altitudes/depths (*lower panels*) from a supernova explosion associated with the 2.5Myr old  $^{60}\text{Fe}$  peak deposits. The figures show our results for the two different associations (same color code for the associations as in Figure 1). *Left panels:* SN associated with Tucana Horologium (70 pc). *Right panels:* SN associated with Upper Centaurus Lupus (140 pc). The diffusion coefficient assumed here is  $10^{26.5} \text{ cm}^2 \text{ s}^{-1}$  at 10 GeV and follows a Kraichan energy dependence ( $\eta = 0.5$ ). Our best fit to the observed spectra is given by the *dashed* and *dotted* lines in the upper panels for the two distinct SN sites (*left* and *right* panels). The reader is refer to the text for a discussion of all the separate contributions expected to the total cosmic-ray spectra (*dashed black line*).

both spectral figures, the *black dashed* line depicts the entire combined cosmic ray energy spectrum.

Lastly, a straightforward fit to the lower and higher (extragalactic) energy components of the cosmic-ray spectrum, which we add to our PeVatron contribution, allows us to estimate the total average cosmic radiation dose experienced at Earth (*bottom panels* in Figures 3 and 4). The absorbed dose rates are given in units of mGy/yr ( $1\text{mGy/yr} \approx 3.2 \times 10^{-11} \text{ watt/kg}$ ). The upper edge of the *grey shaded area* in the lower

panels of Figures 3 and 4 represents the average dose rate during the first  $10^4$  years after explosion and the lower edge during the first  $10^5$  years. We also show in *violet* colors the polarized muon component which is the dominant contribution of the cosmic radiation dose at ground level and is 100% of the dose after 10 meter-water-equivalent (m.w.e.) below the surface.

In brief, we find that a SN explosion in the Sco-Cen association (140 parsecs away) is expected to have raised the level

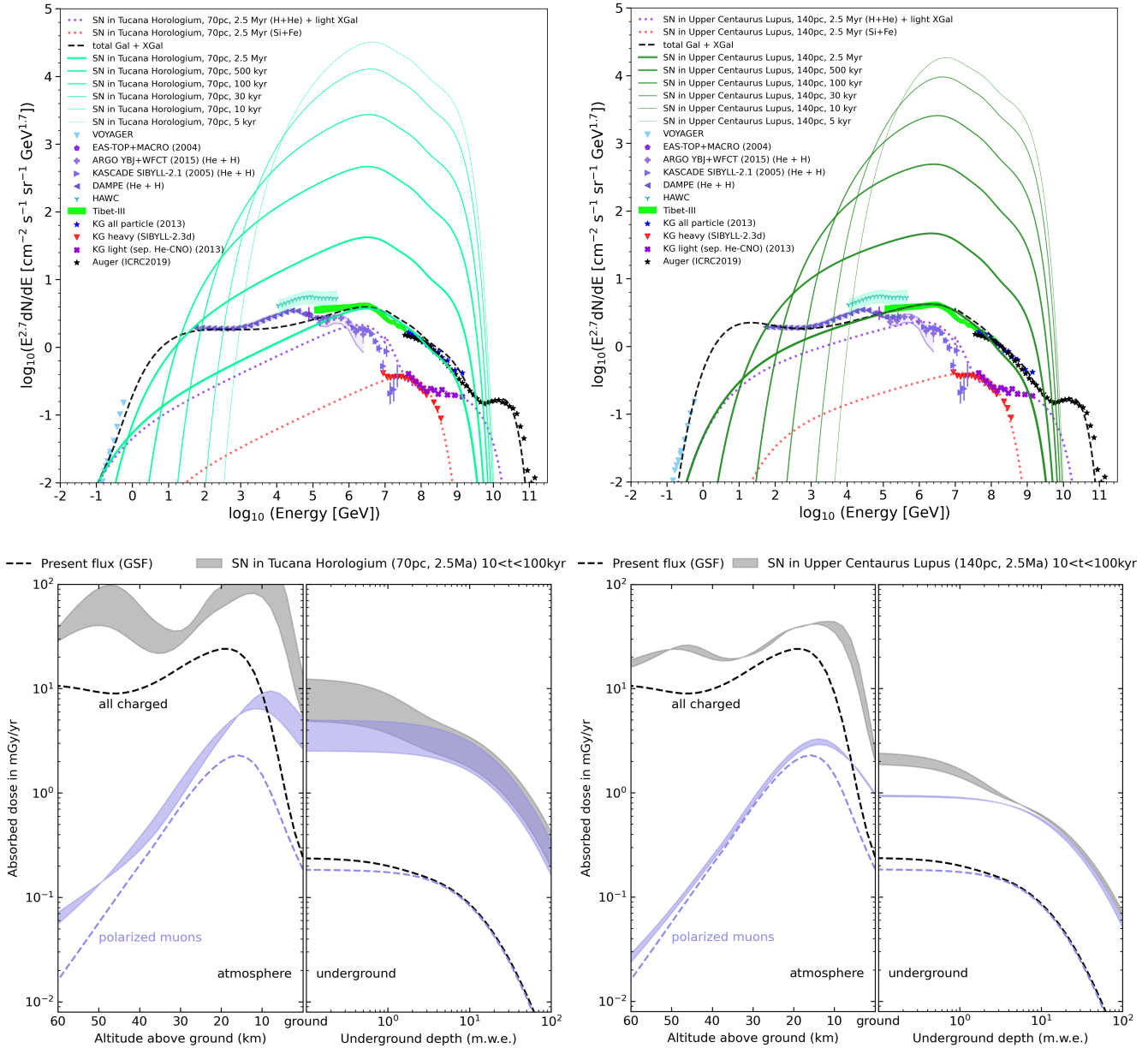


**Figure 4.** Same as Fig. 3 but with a diffusion coefficient assumed to be  $10^{27} \text{ cm}^2 \text{ s}^{-1}$  at 10 GeV.

of cosmic radiation by a factor  $\approx 2$  ( $\approx 10$ ) for about 100 kyr, while a supernova in Tuc-Hor (70 parsecs away) raised it by a factor  $\approx 10$  ( $\approx 30$ ) for about 100 kyr, for  $D_0 = 10^{26.5} (10^{27}) \text{ cm}^2 \text{ s}^{-1}$ . In the section that follows we discussed the consequences that this most recent SN event would have had in terms of past climate and, in particular, in the evolution of organisms on Earth.

## 5. DISCUSSION

The geological record regarding the variations in  $^{60}\text{Fe}$  concentration indicate that a SN exploded near the Earth about 2.5 Myr ago. The discovery of a new “bubble” remnant and a runaway star give credence to the idea that this SN explosion likely originated from the Upper Centaurus Lupus, a sub-

group of the OB association Sco-Cen, 140 pc away in the direction of the Galactic center.

Interestingly, the phase-flip anisotropy at 100 TeV in the direction of Upper Centaurus Lupus (Figure 1) indicates, as we argued here, that the SN that synthesized the  $^{60}\text{Fe}$ , was likely also a PeVatron source. A lone PeVatron source in the OB association Sco-Cen would, at the same time, dominate the flux in the 100 TeV - 5 PeV range today and be responsible for synthesizing the  $^{60}\text{Fe}$  sediments about 2.5 Myrs ago, which were then swiftly transported to the surface of Earth (Ertel et al. 2023). Since the older Tuc-Hor stellar association was also widely discussed as a possible SN candidate, we also consider it here for the sake of completeness. The

observational data on cosmic-ray flux and composition in the knee region allows us to effectively constrain the physical parameters of our SN model and provide a realistic estimate of the radiation doses at various times since the SN explosion took place. Our results are tellingly summarized in Figures 3 and 4.

The probability for a nearby SN occurrence is increased because the Solar System recently entered the LB. Fifteen SN explosions are estimated to have occurred in order to inflate the LB over the last 15 million years (Benítez et al. 2002; Ertel et al. 2023). We know from the reconstruction of the LB history (Zucker et al. 2022) that at least 9 SN exploded during the past 6 Myrs. This gives about one SN every  $\approx 6.6 \times 10^5$  years at a distance less than 150 pc. Assuming that the filling factor of stellar clusters in the LB is  $f$ , the SN rate in the LB can then be written as  $\approx 2 \times 10^{-3} f \text{ kpc}^{-2} \text{ yr}^{-1}$ . This simple estimate agrees well with the historical SN rate for  $f \approx 0.1$ , which gives approximately 1 event every 50 years in our Galaxy.

The results presented here for the expected cosmic-ray flux from a nearby SN differ from those described in Melott et al. (2017), which we have used previously in Globus et al. (2021). The reason is twofold. First, they assume a distance of 50 pc, while we now know that Tuc-Hor was further away ( $\approx 70$  pc) at the time of the SN explosion. Second, they presume  $2.5 \times 10^{50}$  erg in cosmic rays and a spectral index of 2.2, with a cutoff at 1 PeV. Here we show that to actually fit the knee region of the cosmic-ray spectrum, one needs  $\approx 10^{49}$  erg in cosmic rays (which is the same order of magnitude as the  $\gamma$ -ray luminosity in SNRs) and a cutoff at 5 or 6 PeV (to effectively capture the knee). We also show that the spectral shape varies with time and this needs to be taken into account when calculating the corresponding doses (Figures 3 and 4). We find lower average doses as calculated over extended periods of time. That is,  $\approx 10$  mGy/yr during the first  $10^4$  yrs after a SN explosion in Tuc-Hor and  $\approx 3$  mGy/yr during the first  $10^4$  yrs after a SN explosion in Sco-Cen (UCL).

It is not clear what would the biological effects of such radiation doses be. The study of populations living in Kerala, India, where the background radiation level was observed to vary between 0.1 and 45.0 mGy/yr showed that 5.0 mGy/yr (mean dose) may be the threshold dose for double strand break induction (Jain et al. 2016). Double strand breaks in DNA can potentially lead to mutations and jump in the diversification of species. Costa et al. (2024) showed that the rate of virus diversification in the African Tanganyika lake accelerated 2-3 Myr ago. It would be appealing to better understand whether this can be attributed to the increase in cosmic-radiation dose we predict to have taking place during that period. We note that the calculated dose from a SN occurring in Tuc-Hor, whose properties can account for the  $^{60}\text{Fe}$  concentration peak 2.5 Myr ago as well as describe the cosmic-ray spectrum and composition in the knee region, would certainly not induce a mass extinction. On the other

hand, it could lead to a diversification of species through an increase in the mutation rate.

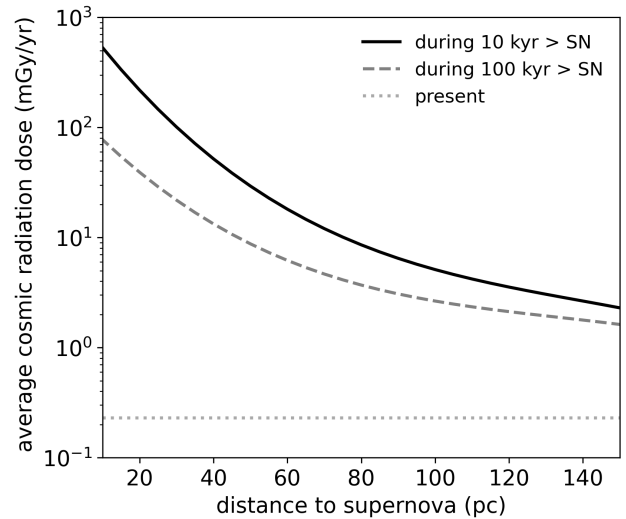


**Figure 5.** The average dose rate experience at ground level as a function of the distance to the early SN. The average dose is calculated over the first 10 kyr (solid line) and over the first 100 kyr (dashed line) after the SN explosion. The total energy released in cosmic rays is assumed here to be  $10^{49}$  erg. The diffusion coefficient is  $10^{27} \text{ cm}^2 \text{ s}^{-1}$  at 10 GeV. The current dose rate today is indicated by the dotted line.

By way of comparison, a radiation dose for a SN occurring at 10 pc (considering the same rate as above, which gives one event approximately every 150 Myr), assuming a diffusion coefficient of  $10^{27} \text{ cm}^2 \text{ s}^{-1}$  and a total energy of  $10^{49}$  erg in cosmic rays, gives an average radiation dose of 600 mGy/yr, which has been calculated averaging over the first 10 kyr. We refer the reader to Figure 5, where we present the average dose as a function of SN distance under the same stated assumptions. The dose limit for occupational exposure in a nuclear facility is, for comparative purposes, 500 mSv/yr for the skin and extremities.<sup>4</sup>

It is therefore certain that cosmic radiation is a key environmental factor when assessing the viability and evolution of life on Earth, and the key question pertains to the threshold for radiation to be a favorable or harmful trigger when considering the evolution of species. The exact threshold can only be established with a clear understanding of the biological effects of cosmic radiation (especially muons that dominate at ground level), which remains highly unexplored.

We finally remark that in our model the “knee” in the cosmic-ray spectrum, which is due to a nearby SN, is an ephemeral structure. This structure is essential for placing stringent constraints on the cosmic-ray energy content of the PeVatron source as well as on the cosmic-ray diffusion coefficient. We predict that the anisotropy in the PeV range,

<sup>4</sup> 1 mSv/yr  $\approx$  1 mGy/yr for photons and leptons.



is in the direction of one of the nearby stellar associations that is responsible for hosting the nearby SN. Another forecast we make is that the direction of the anisotropy should not change between 100 TeV and 100 PeV as this is the energy at which the Galactic to extragalactic transition commences. As such, cosmic rays play a key role in the development of life on Earth by potentially influencing the mutation rate of early life forms and, as such, potentially assisting in the evolution of complex organisms (e.g., Jain et al. 2016) as well as even shaping the “handedness” of biological molecules (Globus & Blandford 2020).

#### ACKNOWLEDGEMENTS

We thank Roger Blandford, Anne Kolborg, Mordecai-Mark Mac Low, Igor Moskalenko, Theo O’Neill, Mehrnoosh

Tahani, Myriam Telus, Angela Twum for helpful discussions and encouragements. C.N. is grateful to Yulianna Ortega, Xingci Situ, Felix Perez for their support and encouragement through the years. We thank Anatoli Fedynitch for his important contributions to our previous work. We acknowledge grants by the Sloan Foundation (G-2023-19591), the Simons Foundation and the Heising-Simons Foundation. This work was catalyzed during the UCSC STEM Diversity Program and Lamat REU program (CN). UCSC STEM Diversity Program is supported through UNIVERSITY OF CALIFORNIA © Regents of the University of California- UC LEADS. The Lamat REU program is supported by NSF grant 2150255.

#### REFERENCES

- Abeysekera, A. U., Albert, A., Alfaro, R., et al. 2017, *Science*, 358, 911, doi: [10.1126/science.aan4880](https://doi.org/10.1126/science.aan4880)
- Ackermann, M., Ajello, M., Allafort, A., et al. 2011, *Science*, 334, 1103, doi: [10.1126/science.1210311](https://doi.org/10.1126/science.1210311)
- Aglietta, M., Alessandro, B., Antonioli, P., et al. 2004, *Astroparticle Physics*, 20, 641, doi: [10.1016/j.astropartphys.2003.10.004](https://doi.org/10.1016/j.astropartphys.2003.10.004)
- Aharonian, F. A., & Atoyan, A. M. 1996, *A&A*, 309, 917
- Alemanno, F., Altomare, C., An, Q., et al. 2024, *PhRvD*, 109, L121101, doi: [10.1103/PhysRevD.109.L121101](https://doi.org/10.1103/PhysRevD.109.L121101)
- Allen, G. 1999, in *International Cosmic Ray Conference*, Vol. 3, 26th International Cosmic Ray Conference (ICRC26), Volume 3, 480, doi: [10.48550/arXiv.astro-ph/9908209](https://doi.org/10.48550/arXiv.astro-ph/9908209)
- Amenomori, M., Bi, X. J., Chen, D., et al. 2008, *ApJ*, 678, 1165, doi: [10.1086/529514](https://doi.org/10.1086/529514)
- Antoni, T., Apel, W. D., Badea, A. F., et al. 2005, *Astroparticle Physics*, 24, 1, doi: [10.1016/j.astropartphys.2005.04.001](https://doi.org/10.1016/j.astropartphys.2005.04.001)
- Apel, W. D., Arteaga-Velázquez, J. C., Bekk, K., et al. 2011, *PhRvL*, 107, 171104, doi: [10.1103/PhysRevLett.107.171104](https://doi.org/10.1103/PhysRevLett.107.171104)
- Bartoli, B., Bernardini, P., Bi, X. J., et al. 2015, *PhRvD*, 92, 092005, doi: [10.1103/PhysRevD.92.092005](https://doi.org/10.1103/PhysRevD.92.092005)
- Benítez, N., Maíz-Apellániz, J., & Canelles, M. 2002, *PhRvL*, 88, 081101, doi: [10.1103/PhysRevLett.88.081101](https://doi.org/10.1103/PhysRevLett.88.081101)
- Berger, M. J., Coursey, J., Zucker, M., & Chang, J. 2017, *NIST Standard Reference Database 124 (Version 2.0.1)*, doi: [10.18434/T4NC7P](https://doi.org/10.18434/T4NC7P)
- Costa, V. A., Ronco, F., Mifsud, J. C., et al. 2024, *Current Biology*, 34, 1247, doi: <https://doi.org/10.1016/j.cub.2024.02.008>
- Cristofari, P. 2021, *Universe*, 7, 324, doi: [10.3390/universe7090324](https://doi.org/10.3390/universe7090324)
- Dampe Collaboration. 2022, *Science Bulletin*, 67, 2162, doi: [10.1016/j.scib.2022.10.002](https://doi.org/10.1016/j.scib.2022.10.002)
- Dembinski, H., Engel, R., Fedynitch, A., et al. 2017, in *International Cosmic Ray Conference*, Vol. 301, 35th International Cosmic Ray Conference (ICRC2017), 533, doi: [10.22323/1.301.0533](https://doi.org/10.22323/1.301.0533)
- Egger, R. J., & Aschenbach, B. 1995, *A&A*, 294, L25, doi: [10.48550/arXiv.astro-ph/9412086](https://doi.org/10.48550/arXiv.astro-ph/9412086)
- Ellis, J., & Schramm, D. N. 1995, *Proceedings of the National Academy of Science*, 92, 235, doi: [10.1073/pnas.92.1.235](https://doi.org/10.1073/pnas.92.1.235)
- Ertel, A. F., Fry, B. J., Fields, B. D., & Ellis, J. 2023, *ApJ*, 947, 58, doi: [10.3847/1538-4357/acb699](https://doi.org/10.3847/1538-4357/acb699)
- Fang, K., Bi, X.-J., & Yin, P.-F. 2020, *The Astrophysical Journal*, 903, 69, doi: [10.3847/1538-4357/abb8d7](https://doi.org/10.3847/1538-4357/abb8d7)
- Fedynitch, A., Engel, R., Gaisser, T. K., Riehn, F., & Stanev, T. 2015, in *European Physical Journal Web of Conferences*, Vol. 99, European Physical Journal Web of Conferences, 08001, doi: [10.1051/epjconf/20159908001](https://doi.org/10.1051/epjconf/20159908001)
- Frisch, P. C., Redfield, S., & Slavin, J. D. 2011, *Annual Review of Astronomy and Astrophysics*, 49, 237, doi: [10.1146/annurev-astro-081710-102613](https://doi.org/10.1146/annurev-astro-081710-102613)
- Fry, B. J., Fields, B. D., & Ellis, J. R. 2015, *ApJ*, 800, 71, doi: [10.1088/0004-637X/800/1/71](https://doi.org/10.1088/0004-637X/800/1/71)
- Fuchs, B., Breitschwerdt, D., de Avillez, M. A., Dettbarn, C., & Flynn, C. 2006, *MNRAS*, 373, 993, doi: [10.1111/j.1365-2966.2006.11044.x](https://doi.org/10.1111/j.1365-2966.2006.11044.x)
- Fujii, T. 2024, *arXiv e-prints*, arXiv:2401.08952, doi: [10.48550/arXiv.2401.08952](https://doi.org/10.48550/arXiv.2401.08952)
- Gallegos-Garcia, M., Burkhart, B., Rosen, A. L., Naiman, J. P., & Ramirez-Ruiz, E. 2020, *ApJL*, 899, L30, doi: [10.3847/2041-8213/ababae](https://doi.org/10.3847/2041-8213/ababae)
- Galli, P. A. B., Miret-Roig, N., Bouy, H., Olivares, J., & Barrado, D. 2023, *MNRAS*, 520, 6245, doi: [10.1093/mnras/stad520](https://doi.org/10.1093/mnras/stad520)
- Globus, N., Allard, D., & Parizot, E. 2015, *PhRvD*, 92, 021302, doi: [10.1103/PhysRevD.92.021302](https://doi.org/10.1103/PhysRevD.92.021302)
- Globus, N., & Blandford, R. D. 2020, *ApJL*, 895, L11, doi: [10.3847/2041-8213/ab8dc6](https://doi.org/10.3847/2041-8213/ab8dc6)
- Globus, N., Fedynitch, A., & Blandford, R. D. 2021, *ApJ*, 910, 85, doi: [10.3847/1538-4357/abe461](https://doi.org/10.3847/1538-4357/abe461)
- Herbst, K., Heber, B., Kopp, A., Sternal, O., & Steinhilber, F. 2012, *ApJ*, 761, 17, doi: [10.1088/0004-637X/761/1/17](https://doi.org/10.1088/0004-637X/761/1/17)
- Hoogerwerf, R., de Bruijne, J. H. J., & de Zeeuw, P. T. 2000, *ApJL*, 544, L133, doi: [10.1086/317315](https://doi.org/10.1086/317315)
- Hörandel, J. R. 2003, *Astroparticle Physics*, 19, 193, doi: [10.1016/S0927-6505\(02\)00198-6](https://doi.org/10.1016/S0927-6505(02)00198-6)
- Hyde, M., & Pecaut, M. J. 2018, *Astronomische Nachrichten*, 339, 78, doi: <https://doi.org/10.1002/asna.201713375>
- Jain, V., Kumar, P. V., Koya, P., Jaikrishan, G., & Das, B. 2016, *Mutation Research/Fundamental and Molecular Mechanisms of Mutagenesis*, 788, 50
- Kang, D., Arteaga-Velázquez, J. C., Bertaina, M., et al. 2023, *arXiv e-prints*, arXiv:2312.05054, doi: [10.48550/arXiv.2312.05054](https://doi.org/10.48550/arXiv.2312.05054)
- Karam, P. A., & Leslie, S. A. 1999, *Health physics*, 77, 662
- Kolborg, A. N., Martizzi, D., Ramirez-Ruiz, E., et al. 2022, *ApJL*, 936, L26, doi: [10.3847/2041-8213/ac8c98](https://doi.org/10.3847/2041-8213/ac8c98)
- Kolborg, A. N., Ramirez-Ruiz, E., Martizzi, D., Macias, P., & Soares-Furtado, M. 2023, *ApJ*, 949, 100, doi: [10.3847/1538-4357/acca80](https://doi.org/10.3847/1538-4357/acca80)
- Kuznetsov, M. Y., Petrov, N. A., Plokhikh, I. A., & Sotnikov, V. V. 2024, *JCAP*, 2024, 125, doi: [10.1088/1475-7516/2024/05/125](https://doi.org/10.1088/1475-7516/2024/05/125)
- Lhaaso Collaboration. 2024, *Science Bulletin*, 69, 449, doi: [10.1016/j.scib.2023.12.040](https://doi.org/10.1016/j.scib.2023.12.040)

- Lingenfelter, R. E. 2018, *Advances in Space Research*, 62, 2750, doi: [10.1016/j.asr.2017.04.006](https://doi.org/10.1016/j.asr.2017.04.006)
- Maíz-Apellániz, J. 2001, *ApJL*, 560, L83, doi: [10.1086/324016](https://doi.org/10.1086/324016)
- Malkov, M. A., & Moskalenko, I. V. 2022, *ApJ*, 933, 78, doi: [10.3847/1538-4357/ac7049](https://doi.org/10.3847/1538-4357/ac7049)
- Mamajek, E. E. 2016, in *Young Stars & Planets Near the Sun*, ed. J. H. Kastner, B. Stelzer, & S. A. Metchev, Vol. 314, 21–26, doi: [10.1017/S1743921315006250](https://doi.org/10.1017/S1743921315006250)
- Meighen-Berger, S., & Li, M. 2019, in *International Cosmic Ray Conference*, Vol. 36, 36th International Cosmic Ray Conference (ICRC2019), 961. <https://arxiv.org/abs/1910.05984>
- Melott, A. L., Thomas, B. C., Kachelrieß, M., Semikoz, D. V., & Overholt, A. C. 2017, *ApJ*, 840, 105, doi: [10.3847/1538-4357/aa6c57](https://doi.org/10.3847/1538-4357/aa6c57)
- Morales-Soto, J. A., & Arteaga-Velázquez, J. C. 2022, arXiv e-prints, arXiv:2208.14245, doi: [10.48550/arXiv.2208.14245](https://doi.org/10.48550/arXiv.2208.14245)
- Nimmo, F., Primack, J., Faber, S. M., Ramirez-Ruiz, E., & Safarzadeh, M. 2020, *ApJL*, 903, L37, doi: [10.3847/2041-8213/abc251](https://doi.org/10.3847/2041-8213/abc251)
- Particle Data Group. 2020, *Progress of Theoretical and Experimental Physics*, 2020, 083C01, doi: [10.1093/ptep/ptaa104](https://doi.org/10.1093/ptep/ptaa104)
- Piecka, M., Hutschenreuter, S., & Alves, J. 2024, arXiv e-prints, arXiv:2407.13226, doi: [10.48550/arXiv.2407.13226](https://doi.org/10.48550/arXiv.2407.13226)
- Ratzenböck, S., Großschedl, J. E., Alves, J., et al. 2023, *A&A*, 678, A71, doi: [10.1051/0004-6361/202346901](https://doi.org/10.1051/0004-6361/202346901)
- Robitaille, J. F., Scaife, A. M. M., Carretti, E., et al. 2018, *A&A*, 617, A101, doi: [10.1051/0004-6361/201833358](https://doi.org/10.1051/0004-6361/201833358)
- Rosen, A. L., Lopez, L. A., Krumholz, M. R., & Ramirez-Ruiz, E. 2014, *MNRAS*, 442, 2701, doi: [10.1093/mnras/stu1037](https://doi.org/10.1093/mnras/stu1037)
- Schulreich, M. M., Feige, J., & Breitschwerdt, D. 2023, *A&A*, 680, A39, doi: [10.1051/0004-6361/202347532](https://doi.org/10.1051/0004-6361/202347532)
- Standard Atmosphere, U. S. 1976, US Gov. Print. Off., Washington, DC
- Vieu, T., & Reville, B. 2023, *MNRAS*, 519, 136, doi: [10.1093/mnras/stac3469](https://doi.org/10.1093/mnras/stac3469)
- Wallner, A., Froehlich, M. B., Hotchkis, M. A. C., et al. 2021, *Science*, 372, 742, doi: [10.1126/science.aax3972](https://doi.org/10.1126/science.aax3972)
- Weaver, R., McCray, R., Castor, J., Shapiro, P., & Moore, R. 1977, *ApJ*, 218, 377, doi: [10.1086/155692](https://doi.org/10.1086/155692)
- Zucker, C., Goodman, A. A., Alves, J., et al. 2022, *Nature*, 601, 334, doi: [10.1038/s41586-021-04286-5](https://doi.org/10.1038/s41586-021-04286-5)